

All Electrical NZFMR Magnetometry up to 500°C Using SiC Devices

F. Sgrignuoli ^{*1}, I. Viti ¹, Z.G. Yu ¹, E. Albright ², P. Lenahan ², S. Goswami ³,
R. Ghandi ³, M. Aghayan ³, and D.M.Shaddock³

¹ QuantCAD LLC, 5235 S. Harper Ct., Chicago IL, 60615, USA

² The Pennsylvania State University, University Park, PA, 16802, USA

³ GE Aerospace Research Center, 1 Research Cir, Niskayuna, NY, 12309, USA

* fabrizio.sgrignuoli@quantcad.com

Keywords: Quantum magnetometry, NZFMR, high temperature, SiC diodes

Abstract.

Silicon Carbide (SiC) is renowned for its exceptional thermal stability, making it a crucial material for high-temperature power devices in extreme environments. While optically detected magnetic resonance (ODMR) in SiC has been widely studied for magnetometry, it requires complex setups involving optical and microwave sources. Similarly, electrically detected magnetic resonance (EDMR) in SiC, which relies on an electrical readout of spin resonance, has also been explored for magnetometry. However, both techniques require microwave excitation, which limits their scalability. In contrast, SiC's spin-dependent recombination (SDR) currents enable a purely electrical approach to magnetometry through the near zero-field magnetoresistance (NZFMR) effect, where the device resistance changes in response to small magnetic fields. Despite its potential, NZFMR remains underexplored for high-temperature applications. In this work, we demonstrate the use of NZFMR in SiC diodes for high-temperature magnetometry and achieve sensitive detection of weak magnetic fields at temperatures up to 500°C. Our technology offers a simple and cost-effective alternative to other magnetometry architectures. The NZFMR signal is modulated by an external magnetic field, which alters the singlet-triplet pair ratio controlled by hyperfine interactions between nuclear and electron/hole spins as well as dipole-dipole/exchange interactions between electron and hole spins, providing a novel mechanism for magnetometry sensing at elevated temperatures. A critical advantage of our approach is its low power consumption—less than 0.5 W at 500°C for magnetic fields below 5 Gauss. This approach provides a sensitive, reliable, and scalable solution with promising applications in space exploration, automotive systems, and industrial sectors, where high performance in extreme conditions is essential.

Introduction

Due to its unique thermal, mechanical, and electronic properties, SiC has emerged as a crucial material in high-power electronics and devices designed for operation in harsh environments. Its wide bandgap (approximately 3.2 eV for 4H-SiC) allows SiC to sustain high electric fields, high voltages, efficient heat dissipation, and operate at temperatures far exceeding those of silicon-based devices [1]. These attributes make this material indispensable in applications requiring durability and efficiency under extreme conditions, such as power electronics, automotive systems, smart grids, and aerospace [2-4], to cite a few. Additionally, SiC hosts defects that exhibit optically and electrically

active spin states, making it a versatile material for quantum sensing and spintronics [5-11]. Unlike nitrogen-vacancy (NV) centers in diamonds, SiC defects are compatible with modern semiconductor fabrication techniques, offering a scalable platform for quantum technologies [5, 11].

A concrete example of SiC's pivotal role lies in small-size, weight, and power consumption (SWaP) magnetometry for high-temperature environments, crucial for applications ranging from engine monitoring and chip quality control to space exploration [12-14]. Conventional magnetometers, such as fluxgates, face significant limitations in size, power consumption, and susceptibility to thermal noise [14]. Fluxgate magnetometers also require frequent calibration and are prone to performance degradation due to noise interference [14]. ODMR techniques have introduced high sensitivity for magnetic field detection at smaller scales [15]. However, ODMR systems, such as optically pumped magnetometry (OPM), rely on microwave excitation and optical detection, complicating their integration into SWaP devices [14]. Similarly, EDMR, which monitors spin-dependent phenomena by detecting changes in electrical current, improves signal readout but still requires microwave fields, limiting its practicality in miniaturized devices [16]. These techniques also struggle to function in high-temperature environments, with fluxgates degrading above 150-200°C [17], OPMs suffering from instability in atomic vapor cells [18], and EDMR experiencing reduced spin coherence and increased thermal noise [19].

Near-zero-field magnetoresistance (NZFMR) is emerging as a powerful defect metrology alternative [20-23], overcoming many of the limitations of traditional magnetometry [14]. NZFMR does not require microwave sources or large magnetic fields, significantly reducing system complexity, power consumption, and cost [24]. By avoiding RF fields, NZFMR enables spectroscopy below metallization layers to detect point defects in fully processed semiconductor devices, making it highly valuable for integrated circuit reliability [23]. Moreover, NZFMR allows for self-calibrating magnetometry [14]. Similar to EDMR, NZFMR involves spin-dependent changes in current, but instead of relying on resonance at higher fields, the change is centered at near-zero magnetic fields. Low-field hyperfine mixing and electron-electron dipolar interactions alter the singlet-to-triplet pairing ratio in an NZFMR response, enabling the detection of changes in the recombination current with external magnetic field variations [24-26]. Additionally, the magnetic isotopes of host and dopant atoms involved in hyperfine interactions act as natural, stable markers, allowing self-calibration over time and temperature [14]. This stability is rooted in the stable energy levels of SiC's defects, which remain unaffected by temperature fluctuations, ensuring consistent performance across various conditions [6].

By utilizing NZFMR to probe the spin properties of active defects in standard SiC p-n junction devices, we have demonstrated an all-electrical SWaP magnetometry capable of operating at temperatures up to 500°C without isotopic purification or design enhancements. The proposed technology represents a significant advancement, overcoming the limitations of existing magnetometry techniques and opening new avenues for metrology and space exploration. It provides a reliable, scalable, cost-effective solution for extreme environments without sacrificing sensitivity, setting a new standard for high-performance magnetic field sensing across the most challenging conditions.

Methods

The core of our method relies on the near zero-field spin-dependent recombination (SDR) phenomenon, which enables the electrical readout of a current that encodes the magnetic field in which the sensor is immersed. The intrinsic defects of the SiC device dictate the response of the SDR current. When a semiconductor junction device is biased to yield a pronounced recombination current, carriers couple with deep-level (spin-dependent) defect electrons, as schematized in Fig.1. These spin states can be singlet or triplet states. Due to the Pauli exclusion principle, electron-hole recombination is allowed only in a singlet spin configuration, creating a bottleneck when the pair is in a triplet state. At near-zero magnetic fields, this bottleneck is alleviated by an external magnetic field [25, 26], which flips the defect electron's spin triplet into singlet states. This process remains active despite the thermal energy being orders of magnitude larger than the single-triplet mixing energy.

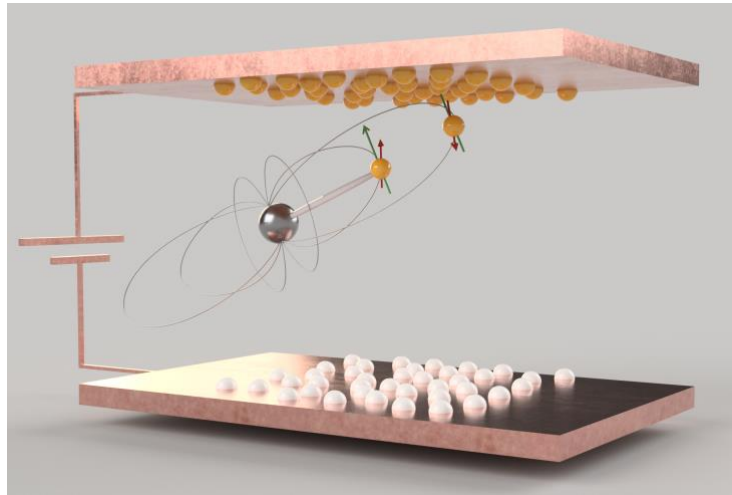


Figure 1: Illustration of the SDR mechanism. A conduction electron (gold sphere) and a trapped electron (gold sphere bound to a defect, represented by a grey sphere) couple to form an intermediate spin state. These spin states can either be singlet or triplet. Due to the Pauli exclusion principle, recombination through triplet states cannot conserve spin angular momentum. However, when the defect electron's spin is 'flipped' through hyperfine mixing or electron-electron dipolar interactions at near-zero magnetic fields, recombination becomes allowed, leading to an increase in the recombination current.

Figure 2 shows our custom experimental setup to detect DC magnetic fields through a conventional SiC diode's response. The proposed technology is based on standard equipment, schematized in Figure 2a, and traditional SiC devices. The proposed technology did not use isotopically purified material, offering a cost-effective solution. The SiC device utilized in this study was, indeed, not designed explicitly for magnetometry operations. It was a lateral p⁺/i/n⁺ diode for high-temperature SiC operations, with an ion-implanted p-well body within a low-doped n-epitaxial region on mis-cut 4H-SiC conductive N⁺ substrate encapsulated with vapor-deposited SiO₂ and Si₃N₄ films. The SiC die was mounted onto a 500°C compatible alumina substrate using gold-nanoparticle sintered pastes, with Au pads and routing lines directly written on the substrate [27-29]. This packaged diode was stacked between two sets of coils [30]. These coils function as nulling and modulation coils. The modulation coils generate alternating magnetic fields driven by an AC signal, which interact with the sample to modulate its magnetization. This modulation induces resonant responses in the sample, which is vital for detecting magnetic transitions. The modulation frequency is carefully chosen to enhance signal sensitivity significantly when suppressing low-frequency noise. Simultaneously, nulling coils generate the DC magnetic field sensed in this work. Additionally, nulling coils will cancel out unwanted background magnetic fields in real-world applications, ensuring the device will operate in a controlled near-zero magnetic field region. Besides their different functionalities, these coils have a 28 AWG cross-sectional area and a field efficiency of 40 Gauss amps [30]. They were connected with ceramic-coated wire, secured with through-hole connectors, and further enhanced with conductive paste to reduce resistance to create the stack shown in Fig. 2b. This assembly is housed within a high-temperature oven, showing full operation even after 60 minutes at 500°C with a current of 2 amps, demonstrating long-operation capabilities.

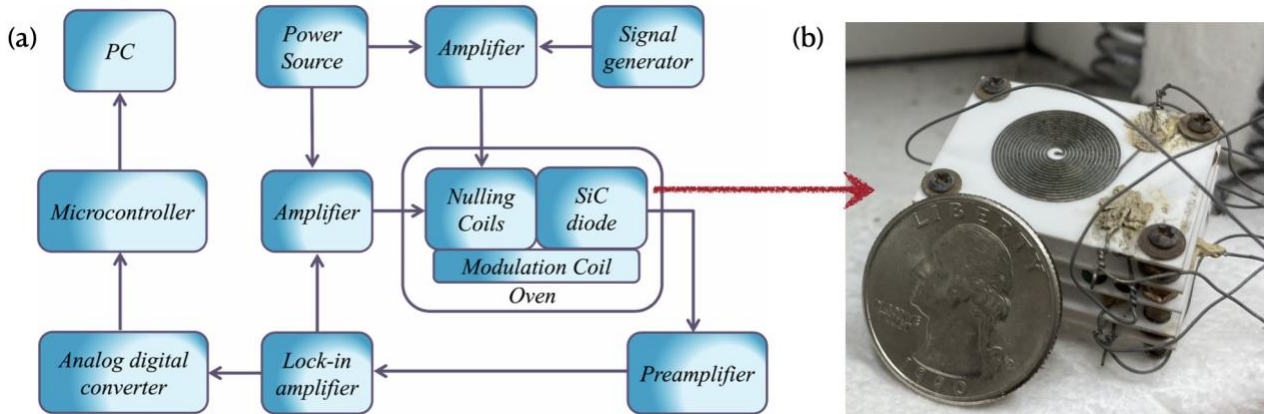


Figure 2: (a) Diagram of the high-temperature magnetometry setup. (b) A SiC diode mounted on a printed circuit board chip stack with modulation and nulling coils, specifically designed to sustain high-temperature operations, formed the assembly placed in the oven. The proposed technology is approximately the size of a quarter, demonstrating a significant reduction in form factor.

To handle the weak signals produced by the SiC diode, a series of amplification and signal processing components are integrated into the setup. The preamplifier strengthens the weak SDR signals, while the lock-in amplifier isolates and enhances the signal of interest by locking onto the modulation frequency. This lock-in technique improves the signal-to-noise ratio, making extracting meaningful data from the noisy environment easier. The lock-in amplifier is tuned to the modulation frequency, allowing selective detection of the resonant responses induced by the alternating magnetic field. The system also includes an analog-to-digital converter (ADC), which converts the amplified analog signal into a digital format for further processing. The microcontroller then manages the data acquisition and processing, adjusting system parameters based on the detected signals in real-time. The PC interface gives the user control over the entire experiment, including setting the modulation and nulling fields and visualizing the magnetic field data collected from the device.

In summary, the combination of high-temperature materials, advanced modulation techniques, and

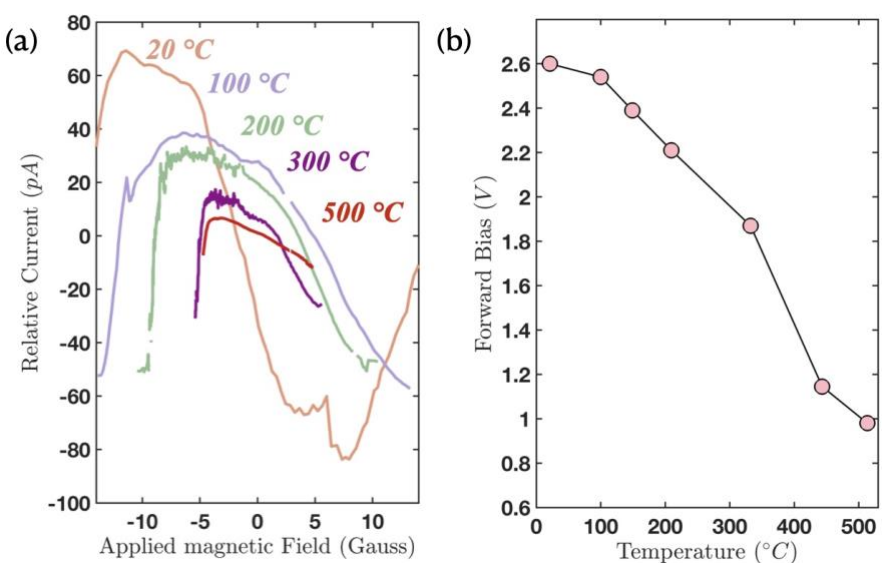


Figure 3: (a) Relative current as a function of the applied magnetic field at different temperatures. 500 °C data are multiplied by a factor of 2 to increase visibility. (b) Forward bias-voltage as a function of temperature. These data are obtained by fixing the diode current to 200 nA for all the different temperatures.

sensitive detection makes the system reported in Fig.2 suitable for robust DC magnetometry in extreme conditions. Significantly, our setup is not limited to DC detection. By adequately changing the electronics and the features of our lock-in amplifier to detect signals with frequencies below 0.1 Hz, we can also extend our method to detect AC magnetic fields.

Results and Discussions

Figure 3 reports averaged NZFMR signals (panel a) and forward bias (panel b) measurements for different temperatures. NZFMR signals exhibit a clear shift as the temperature increases, with the relative current showing a progressive change across the magnetic field range. As the temperature rises, the SiC device becomes more conductive. Indeed, the bias voltage is reduced to maintain a constant current of 200nA on a SiC diode, which helps minimize thermal effects. Without averaging the current, the temperature-induced drift would obscure the NZFMR signal, making it challenging to distinguish magnetic field-related variations. Even though the NZFMR signal weakens at higher temperatures (see Fig. 3a), the relationship between the magnetic field and current remains evident, confirming the system's ability to detect NZFMR under extreme thermal conditions. Also, power consumption increases slightly at 500°C due to an increase in coil resistivity from 0.5Ω at 20°C to 1.2Ω at 500 °C. Still, it remains low: lower than 0.5 W for fields less than 5 Gauss. Therefore, the proposed technology operates at low power, reflecting the vision of a robust SWaP all-electrical magnetometer on-chip to hostile environments.

Figure 4 demonstrates how an applied offset magnetic field impacts NZFMR measurements and device sensitivity. Panel (a) shows NZFMR signals acquired at 500°C under different offset magnetic fields (+1.5 Gauss, 0 Gauss, and -1.5 Gauss), revealing a systematic vertical shift in the relative current as the offset field is increased or decreased. This shift indicates a clear correlation between a varying magnetic environment and the relative current response, demonstrating NZFMR magnetometry at high temperatures. Panel (b) presents the device's sensitivity as a function of bandwidth for various temperatures, estimated using the following relation:

$$\frac{\delta B}{\sqrt{\Delta f}} = 2\sigma\sqrt{\pi q} \frac{\sqrt{I_0}}{\Delta I} \quad (1)$$

where q is the electronic charge, I_0 is the DC current responsible for the flicker noise, Δf is the measurement bandwidth, ΔI is the current change, and σ is the signal line width [14]. As the bandwidth increases, the system's sensitivity decreases because more noise is introduced over a broader range of frequencies, which lowers the signal-to-noise ratio and makes it harder to detect small changes in the magnetic field.

Simultaneously, panel (b) also shows a temperature dependence, with lower temperatures yielding better sensitivity. This behavior is due to increased thermal noise, raising the temperature. This reduction in sensitivity at elevated temperatures is

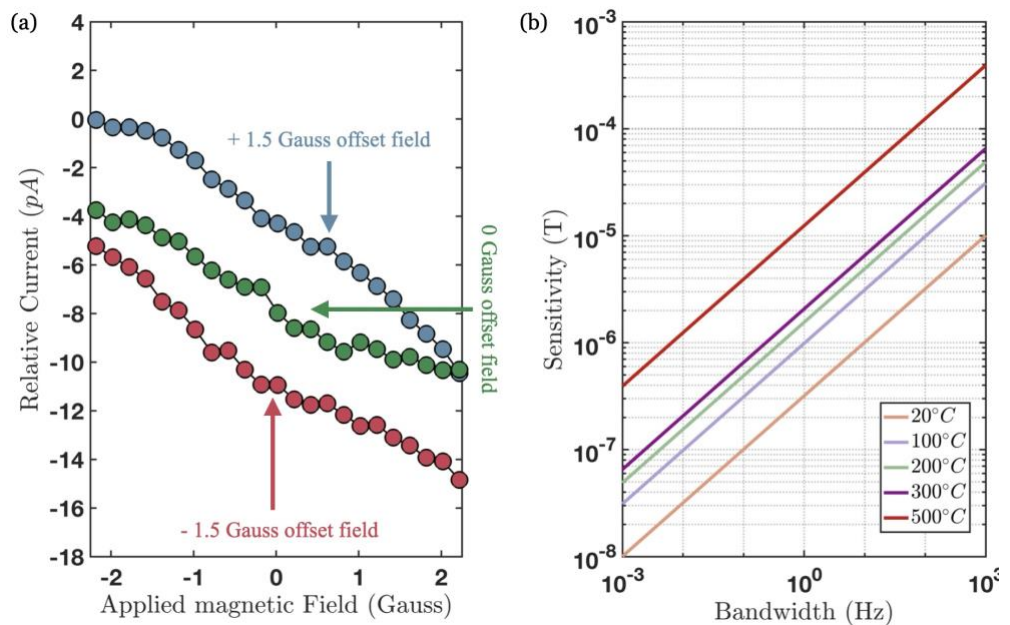


Figure 4: (a) Change in the device current with the magnetic field. Data are taken at 500 °C. Each curve has an average of twenty runs. (b) Magnetometry sensitivity as a function of the bandwidth for different temperatures.

primarily driven by two factors: the broadening of the NZFMR signal (i.e., σ) and a decrease in the current response (i.e., ΔI) to magnetic fields. As temperature increases, the linewidth of the NZFMR signal widens, resulting from enhanced phonon interactions and increased scattering between charge carriers and lattice defects in the SiC diode. This broadening reduces the ability to distinguish small magnetic field changes as the signal becomes less defined. Additionally, higher temperatures reduce the current response to applied magnetic fields due to increased carrier recombination and thermal excitations that compete with the magnetoresistive effect. Despite these factors, the sensitivity reduction is modest (almost two orders of magnitudes), demonstrating that our SiC-based NZFMR sensor remains robust for high-temperature magnetic field detection, even though not specifically designed for magnetometry applications.

Conclusions

In conclusion, our work demonstrates the viability of an all-electrical NZFMR-based magnetometry system utilizing SiC diodes for high-temperature operations. Our technology successfully detects low magnetic fields at temperatures up to 500°C and offers a cost-effective and scalable solution. A commercially available SiC diode, not specifically designed for magnetometry, was mounted on a custom-designed stack with modulation and nulling coils engineered for high-temperature resilience. Our high-temperature magnetometer is compact, with the size of a quarter, and consumes less than 0.5 W at 500°C for magnetic fields below 5 Gauss, making it an attractive option for robust, low-SWaP, all-electrical magnetometry in harsh environments.

Several strategies could be used to further improve this system's sensitivity, especially at high temperatures. First, designing SiC diodes specifically for magnetometry by engineering defect states and optimizing doping profiles could enhance the current response ΔI , reducing spin-independent recombination losses at elevated temperatures and, thus, a higher sensitivity. Additionally, using isotopically purified SiC material will minimize hyperfine interactions, leading to a narrower line width σ and an enhanced signal. Furthermore, advanced signal processing techniques, including adaptive filtering and noise reduction algorithms, could extract more accurate signals from noisy environments, improving the overall performance. By implementing these strategies, SiC-based NZFMR magnetometry can achieve superior sensitivity and reliability, positioning it as a leading solution to high-performance magnetic field sensing in extreme environments and a reliable technology for space exploration, automotive systems, and industrial applications.

Acknowledgment

The room-temperature data are based on work supported by the National Aeronautics and Space Administration under Contract No. 80NSSC23CA145 issued through the SBIR/STTR Program. The high-temperature data are based on work supported by the Defense Advanced Research Projects Agency (DARPA) under Agreement No. HR0011-23-9-0114. We acknowledge useful discussions with M. E. Flatté, C. J. Cochrane, and H. Kraus.

References

- [1] S. M. Sze, *Physics of semiconductor devices*, John Wiley & Sons, 2021.
- [2] B. Mietek. "Status and prospects of SiC power devices." *IEEE Transactions on Industry Applications* 126.4 (2006): 391-399.
- [3] J. B. Casady., and R. W. Johnson. "Status of silicon carbide (SiC) as a wide-bandgap semiconductor for high-temperature applications: A review." *Solid-State Electronics* 39.10 (1996): 1409-1422.

- [4] J. D. Spry., et al. "Prolonged 500° C demonstration of 4H-SiC JFET ICs with two-level interconnect." *IEEE Electron Device Letters* 37.5 (2016): 625-628.
- [5] C. P. Anderson, et al. "Electrical and optical control of single spins integrated in scalable semiconductor devices." *Science* 366.6470 (2019): 1225-1230.
- [6] F. W. Koehl, et al. "Room temperature coherent control of defect spin qubits in silicon carbide." *Nature* 479.7371 (2011): 84-87.
- [7] A. Dzurak. "Diamond and silicon converge." *Nature* 479.7371 (2011): 47-48.
- [8] P. V. Klimov, et al. "Electrically driven spin resonance in silicon carbide color centers." *Physical Review Letters* 112.8 (2014): 087601.
- [9] S. Hosung, et al. "Quantum decoherence dynamics of divacancy spins in silicon carbide." *Nature Communications* 7.1 (2016): 12935.
- [10] C. P. Anderson., et al. "Five-second coherence of a single spin with single-shot readout in silicon carbide." *Science Advances* 8.5 (2022): eabm5912.
- [11] D. R. Candido, and M. E. Flatté. "Suppression of the Optical Linewidth and Spin Decoherence of a Quantum Spin Center in a p-n Diode." *PRX quantum* 2.4 (2021): 040310.
- [12] J. L. Phillips, C. T. Russell. "Upper limit on the intrinsic magnetic field of Venus." *Journal of Geophysical Research: Space Physics* 92.A3 (1987): 2253-2263.
- [13] C. T. Russell, et al. "Venus upper atmosphere and plasma environment: Critical issues for future exploration." *GEOPHYSICAL MONOGRAPH-AMERICAN GEOPHYSICAL UNION* 176 (2007): 139.
- [14] C. J. Cochrane, et al. "Vectorized magnetometer for space applications using electrical readout of atomic scale defects in silicon carbide." *Scientific reports* 6.1 (2016): 37077.
- [15] D. Simin et al. "All-optical DC nanotesla magnetometry using silicon vacancy fine structure in isotopically purified silicon carbide." *Physical Review X* 6.3 (2016): 031014.
- [16] M. A., Anders, et al. "Physical nature of electrically detected magnetic resonance through spin-dependent trap assisted tunneling in insulators." *Journal of Applied Physics* 124.21 (2018).
- [17] P. Ripka, "Review of fluxgate sensors." *Sensors and Actuators A: Physical* 33.3 (1992): 129-141.
- [18] D. Budker, and M. Romalis. "Optical magnetometry." *Nature physics* 3.4 (2007): 227-234.
- [19] D. Vuillaume, D. Deresmes, and D. Stievenard. "Temperature-dependent study of spin-dependent recombination at silicon dangling bonds." *Applied physics letters* 64.13 (1994): 1690-1692.
- [20] P. M. Lenahan *et al.*, "Near Zero Field Magnetoresistance Spectroscopy: A New Tool in Semiconductor Reliability Physics". *2023 IEEE International Reliability Physics Symposium (IRPS)*.
- [21] S. J. Moxim *et al.*, "Tunable zero-field magnetoresistance responses in Si transistors: Origin and applications", *J. Appl. Phys.* **135**, 155703 (2024).
- [22] S. J. Moxim, *et al.*, "Near-zero-field magnetoresistance measurements: A simple method to track atomic-scale defects involved in metal-oxide-semiconductor device reliability", *Rev. Sci. Instrum.* **93**, 115101 (2022).
- [23] J. P. Ashton *et al.*, "A New Analytical Tool for the Study of Radiation Effects in 3-D Integrated Circuits: Near-Zero Field Magnetoresistance Spectroscopy", *IEEE Trans. Nuc. Sci.* **66**, 428-436 (2018).
- [24] C. J. Cochrane, and P. M. Lenahan. "Zero-field detection of spin-dependent recombination with direct observation of electron-nuclear hyperfine interactions in the absence of an oscillating electromagnetic field." *Journal of Applied Physics* 112.12 (2012)

- [25] N. J. Harmon, et al. "Spin-dependent capture mechanism for magnetic field effects on interface recombination current in semiconductor devices." *Applied Physics Letters* 123.25 (2023).
- [26] N. J. Harmon, et al. "Modeling of Near Zero-Field Magnetoresistance and Electrically Detected Magnetic Resonance in Irradiated Si/SiO₂ MOSFETs." *IEEE Trans. Nucl. Sci.* **67**, 1669-1673, (2020).
- [27] E. Andarawis, D. Shaddock, S. Goswami, T. Johnson. International Conferences and Exhibition on High Temperature Electronics (HiTEC) (2023))
- [28] D. Shaddock, C. Hoel, J. Hale, M. Poliks, M. Alhendi, F. Alshatnawi, Conference on High Temperature Electronics Network (HiTEN 2022), July , 2022
- [29] M. Östling, R. Ghandi, C.-M. Zetterling, Proc. 2011 IEEE 23rd Intl. Symp. Power, doi: [10.1109/ISPSD.2011.5890778](https://doi.org/10.1109/ISPSD.2011.5890778)
- [30] Patent Pending